Returning now to Eq. (25), we rewrite it, indicating explicitly the dependence on the shifted Fermi momenta, as

$$V(\epsilon)=\sum_{k_i=0}^{k_+}\sum_{k_j=0}^{k_+} a_0(\mathbf{k}_i,\mathbf{k}_j;\,k_+)+\sum_{k_i=0}^{k_-}\sum_{k_j=0}^{k_-} a_0(\mathbf{k}_i,\mathbf{k}_j;\,k_-)$$
$$+\sum_{k_i=0}^{k_+}\sum_{k_j=0}^{k_-}[a_0(\mathbf{k}_i,\mathbf{k}_j;\,k')+a_e(\mathbf{k}_i,\mathbf{k}_j;\,k')]. \quad \text{(A3)}$$

We now carry out an expansion of the amplitudes around k_+, k_-, and $k'=k_F$. Keeping terms to second order in the small parameter ϵ of Eq. (23) and dropping the second derivative of the amplitudes with respect to k_F, we find the result given as the third term of Eq. (32).

To evaluate the integrals in this term, we first make the approximation of setting $\partial a_e/\partial k_F=\partial a_0/\partial k_F$, which can have only a very small effect on the result since $\partial a_e/\partial k_F$ appears with a small coefficient. We also assume (as is true to a good approximation) that a_0 depends only on $|\mathbf{k}_i-\mathbf{k}_j|$. We then can bring the third term in Eq. (32) to the form

$$\frac{4Mp_F}{\pi}\int_0^1 \frac{x^2dx}{k_F{}^3}\left(4-\frac{2x}{k_F}-\frac{2x^3}{k_F{}^3}\right)k_F\frac{\partial}{\partial k_F}a_0(x,k_F), \quad \text{(A4)}$$

where x is the relative momentum.

To carry out the indicated differentiation of a_0 with respect to k_F, we assume a linear dependence of a_0 on k_F and write

$$a_0(x,k_F)=a_0(x,0)+k_Ff(x). \quad \text{(A5)}$$

This linear dependence is verified to a good approximation by the results of the calculations. The function $f(x)$ is then determined by the difference between $a_0(x,0)$, which is the amplitude for zero density or for free particles, and $a_0(x,k_F)$ at the equilibrium density. These amplitudes have been taken from the computed results; evaluation of the integral of Eq. (A4) then gives the value of 0.289 for the third term of Eq. (32).

PHYSICAL REVIEW VOLUME 109, NUMBER 4 FEBRUARY 15, 1958

Measurement of Lattice Vibrations in Vanadium by Neutron Scattering*

C. M. EISENHAUER,† I. PELAH,‡ D. J. HUGHES, AND H. PALEVSKY
Brookhaven National Laboratory, Upton, New York

(Received October 31, 1957)

The energy spectrum of slow neutrons inelastically scattered by vanadium metal has been measured by the time-of-flight technique. The neutrons gain energy by absorbing quanta of lattice vibration energy (phonons). As the nuclear scattering amplitude of vanadium is incoherent, the energy distribution of scattered neutrons is directly related to the frequency distribution of lattice vibrations. The measured neutron energy spectrum, as well as the derived frequency distribution, shows a clearly resolved double peak. This structure, which is distinctly different from the simple Debye distribution, but expected on the basis of detailed calculations, has heretofore not been amenable to direct measurement. The measured frequency distribution is compared with calculations for a body-centered cubic lattice by the Born-von Kármán theory and qualitative agreement is obtained. A more exact comparison awaits measurement of the elastic constants of vanadium.

I. INTRODUCTION

MANY theoretical and experimental studies of the influence of crystal dynamics on the scattering of slow neutrons have been made in recent years. The general theory is discussed by Placzek and Van Hove,[1] who give expressions for the angular and energy distribution of neutrons inelastically scattered by crystals. In this process, phonons (the quanta of lattice vibration energy) may be gained or lost by the neutrons.

The case of single phonon gain by scattering in a cubic crystal is of special interest if the nuclei scatter incoherently (spin-dependent scattering), as the energy gain is simply connected with the frequency distribution of the lattice vibrations of the crystal. Thus a measurement of the emergent energy of slow incident neutrons can be used to obtain the vibration spectrum with little ambiguity. For incoherent inelastic scattering, phonon and neutron properties are related only through the energy conservation condition

$$\hbar^2|k^2-k_0{}^2|/2m=\hbar\omega_j(\mathbf{q}), \quad (1)$$

with no need to satisfy interference (momentum) conditions, as is true for the more frequent case of coherent inelastic scattering. In Eq. (1), $\mathbf{k}$ and $\mathbf{k}_0$ are the scattered and incident neutron wave vectors respectively, m is the neutron mass, and $\omega_j(\mathbf{q})$ the angular frequency of the absorbed or emitted phonon with wave vector $\mathbf{q}$ and polarization index j.

The intensity formula, used to obtain the frequency

* Work carried out under contract with U. S. Atomic Energy Commission.

† Now at National Bureau of Standards, Washington, D. C.

‡ On leave from Weizmann Institute, Rehovoth, Israel, and the Atomic Energy Commission of Israel.

[1] G. Placzek and L. Van Hove, Phys. Rev. 93, 1207 (1954).

distribution of lattice vibrations, has a simple and direct form for the incoherent case. It is expressed as the differential cross section,

$$\frac{d^2\sigma}{d\Omega dk}=\frac{S}{4\pi}\frac{2\hbar k^2}{mMk_0}\exp[-2W]\frac{(\mathbf{k}-\mathbf{k}_0)^2}{|k^2-k_0^2|}$$
$$\times\left[\frac{1}{\exp[\hbar\omega/kT]-1}+\frac{1}{2}(1\pm1)\right]g(\omega). \quad (2)$$

Here S is the bound incoherent scattering cross section per nucleus, M is the ratio of nuclear to neutron mass, $\exp[-2W]$ is the Debye-Waller factor, and $g(\omega)$ is the frequency distribution function, defined as the number of normal vibrations per unit frequency interval divided by the total number of vibrations. The negative or positive sign corresponds to scattering with energy gain or loss, respectively. For a material that scatters incoherently, the energy spectrum of the scattered neutrons in a given direction can be easily converted to the lattice vibration frequency distribution $g(\omega)$ by means of Eq. (2). Furthermore, the spectrum is identical for the case of single crystal and powder scatterers. Although the incoherent scattering has a simple relationship to the vibration spectrum, less information is gained than for the much more complex case of coherent scattering, for which interference conditions as well as energy conservation govern the scattering. However, the simplicity of the incoherent scattering and the direct relationship to $g(\omega)$ means that it is well worth careful investigation at the present time.

Vanadium metal was chosen for this type of measurement as it is cubic (body-centered) and has a scattering cross section that is almost completely incoherent.[2] Earlier attempts have been made to use the inelastic scattering of neutrons to study the lattice vibration of vanadium,[3–5] but the details of the neutron energy spectrum could not be delineated clearly because of insufficient resolving power. The present work at the Brookhaven reactor was performed with higher resolution, in an attempt to establish the details in the vibration spectrum which are expected, in a real crystal, as compared with the simple Debye spectrum.

II. APPARATUS

In the type of experiment in which very slow or "cold" neutrons are inelastically scattered by crystals, the major task is one of obtaining a sufficiently high flux of incident cold neutrons so that a measurable intensity of scattered neutrons is obtained. It is also of importance to attain a very low contamination of faster neutrons in the incident beam.

The cold-neutron facility of the Brookhaven research reactor is shown schematically in Fig. 1. Neutrons from

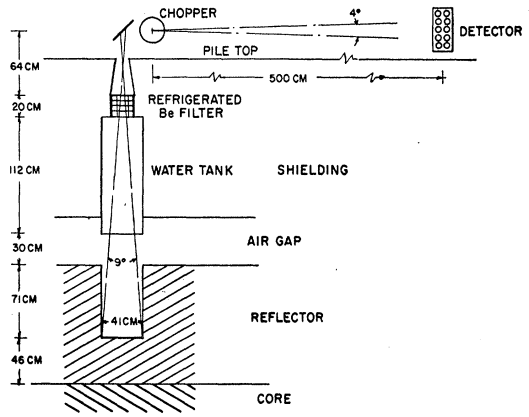

FIG. 1. Cold-neutron facility in the top shield of the Brookhaven research reactor.

the graphite reflector are collimated by concrete and borated paraffin shielding to form an incident beam with a full angular spread of 9° at the sample position. The cadmium ratio, measured with a $1/v$ BF_3 counter, was 200 before the beryllium filter was put into the beam. The 8 in. of refrigerated polycrystalline beryllium filters out neutrons of wavelength less than 3.95 A, primarily by coherent elastic scattering. Neutrons of wavelength $\lambda\geq3.95$ A cannot satisfy the Bragg relation for coherent elastic scattering, and therefore pass through the filter except for a relatively small attenuation caused by thermal inelastic scattering. The latter is reduced by a factor of three by cooling the beryllium to liquid nitrogen temperature. Thus the beam incident on the sample consists in principle only of neutrons with energy below the beryllium cutoff, with an average energy of about 0.0035 ev. Although the neutrons incident on the scatterer are thus not monoenergetic, they are reasonably so, and yet suffer practically no loss in intensity in the filtering process. The usual methods of mechanical or crystal monochromatization would cause a serious decrease in the intensity of neutrons incident on the scatterer.

As a necessary preliminary experiment, the energy distribution of the filtered beam was studied by means of the attenuation of the beam by various thicknesses of gold. The attenuation *vs* thickness curve in gold was consistent with a subthermal component having a Maxwellian flux distribution up to the beryllium cutoff, and a thermal component, with a ratio of thermal to subthermal flux of 1/330. Even as small a thermal contamination as 1/330 in the incident beam, however, produces a significant effect in the scattered neutrons, because of the high elastic scattering for thermal neutrons in vanadium relative to the inelastic scattering of cold neutrons. The action of the filter was therefore studied carefully, and an auxiliary beryllium filter placed between the main filter and the vanadium scatterer to reduce the contamination. A small amount of neutrons was still present near thermal energies,

[2] C. G. Shull and E. O. Wollan, Phys. Rev. **81**, 527 (1951).
[3] B. N. Brockhouse, Can. J. Phys. **33**, 889 (1955).
[4] Carter, Hughes, and Palevsky, Phys. Rev. **104**, 271 (1956).
[5] A. T. Stewart and B. N. Brockhouse, Revs. Modern Phys. **30**, 236 (1958).

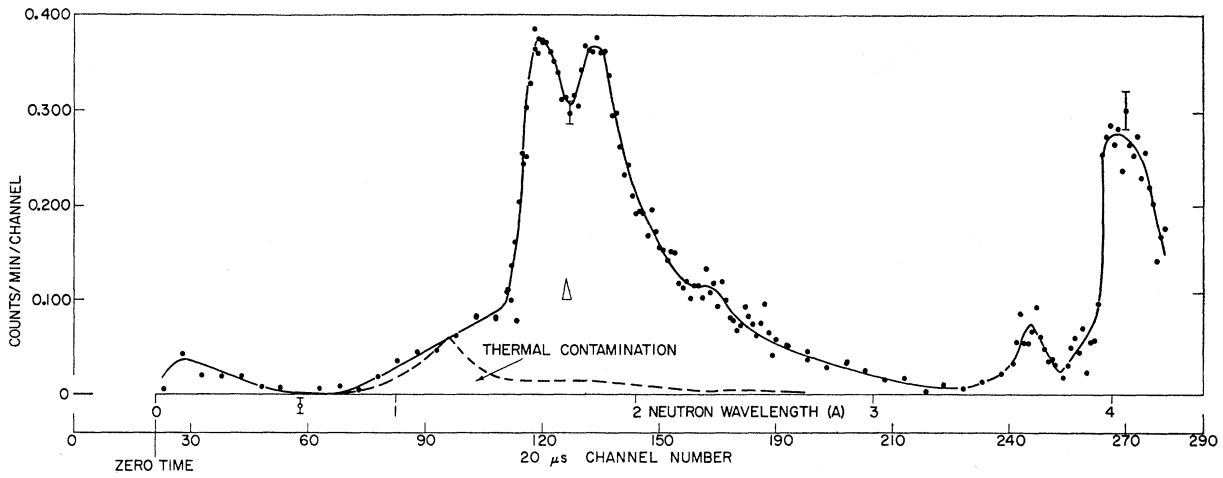

FIG. 2. Time-of-flight spectrum of neutrons scattered from vanadium, with background subtracted. The dashed line shows the estimated contamination from elastic scattering of thermal neutrons in incident beam.

however, probably representing neutrons that had gained energy in the auxiliary filter.

The measured ratio of epicadmium to subthermal neutrons in the filtered beam is 1/6000. However, the effect of epicadmium neutrons at the neutron detector is more serious than would appear from this ratio because of the chopper characteristics, for it reduces the inelastically scattered neutrons by a factor of about 300 while it effectively passes without attenuation the epicadmium neutrons. In addition, the inelastic scattering of vanadium for the cold neutrons is much less than the elastic scattering for the epicadmium neutrons, both of which processes result in neutrons arriving at the detector at the same time.

The velocity spectrum of the neutrons scattered from the vanadium sample was measured by time of flight, using the Brookhaven slow chopper,[6] with a path length of 4.87 meters. A hundred-channel time analyzer, triggered by a magnetic pickup attached to the chopper axis, records a count at the time of arrival of the neutron at the detector. The latter consists of a bank of counters with an efficiency of 60% for 2200-m/sec neutrons. The counters, 14 in number, of 2-in. diameter and 14-in. length, were divided in the sense of rotation of the chopper into three groups delayed with respect to each other to improve time resolution. The channel width of the time analyzer for these measurements was 20 μsec, much larger than any timing uncertainties of the analyzer or the zero time magnetic pickup. The speed for a given run was electronically controlled to about 0.1%. A small and straightforward dead-time correction in the data was necessary at high counting rates as the time analyzer was capable of recording only one count per cycle.

Because of the inherent low intensity of scattered neutrons in an energy gain experiment, careful efforts were made to reduce the background level to as low a rate as possible. The situation was complicated by the fact that the background counting rate of the detector had two components—a flat "room" background from the surrounding facilities of about 0.25 count per minute in each timing channel and a modulated background of about 0.50 count per minute resulting from the epicadmium neutrons in the incident beam. The modulation is caused by the variation of the amount of absorber of the rotor as a function of angle. The counting rate per channel at a peak was about 0.40 count per minute for the operating conditions of 20-μsec timing channels and a 25-μsec burst. It was necessary to make three separate runs so that the entire flight time of interest could be covered with the 100-channel analyzer.

An important source of scattered neutrons is the air in that part of the path of the incident beam that can be seen by the detector. In order to eliminate these neutrons the vanadium sample was placed in a helium atmosphere.

III. MEASUREMENTS AND CORRECTIONS

Because of the low counting rate, it was necessary to run for many hours to obtain sufficient statistical accuracy to establish the detailed structure in the scattered neutron spectrum. Thus Fig. 2, which shows the experimental time-of-flight spectrum of the scattered neutrons after subtraction of the background, represents about 200 hours of operation. The completely automatic nature of the equipment was of great help under these circumstances.

The double-peaked structure in the center of Fig. 2 is the spectrum of inelastically scattered neutrons. The structure is definitely resolved, as can be seen by the resolution triangle shown on the figure. The points to the right of channel 240 display the double break due to neutrons elastically scattered, hence of energy equal to that of the incident neutrons, but with intensities

[6] See D. J. Hughes, *Pile Neutron Research* (Addison-Wesley Press, Cambridge, 1953), pp. 245–9.

severely reduced by the low chopper function in this energy range. The primary break in the elastically scattered neutron spectrum was used to establish the time scale by means of the accurately known wavelength of the cutoff in beryllium (3.95 A). The low-intensity peak in the neighborhood of zero time is due to subthermal neutrons crossing the chopper in the backward direction through spurious openings.

A possible source of error is the thermal component of the incident beam, which, when scattered elastically, arrives at the detector about the same time as the inelastically scattered cold neutrons. The estimated thermal contamination in the measured spectrum, produced by cold neutrons that have gained energy in the auxiliary beryllium filter, is shown in Fig. 2 by the dashed line. The shape was measured by studying the spectrum of cold neutrons scattered from beryllium and the intensity was normalized to the observed intensities at channels 70 through 90, where it was assumed that only the thermal contamination was present.

In order to obtain the spectrum of inelastically scattered neutrons it is necessary to correct the results of Fig. 2 for several additional effects—the loss of neutrons in the sample and in the air path to the detector, the sensitivity of the detector, and the transmission of the chopper or "chopper function." The correction for loss in the sample, which is somewhat involved, is described in Appendix I. The final correction factor, primarily determined by the chopper function, is given in Fig. 3. The relatively large correction at the high-energy end, caused primarily by the chopper function, was checked experimentally by running the spectrum at a higher chopper speed to reduce the correction. The spectrum of inelastically scattered neutrons obtained after application of the final correction factor is given in Fig. 4. The general shape of the curve is changed from the raw data of Fig. 2 but the structure in the results is not affected greatly, the double peak remaining.

Following Squires'[7] treatment of multiphonon scattering, a contribution of about two percent from two-

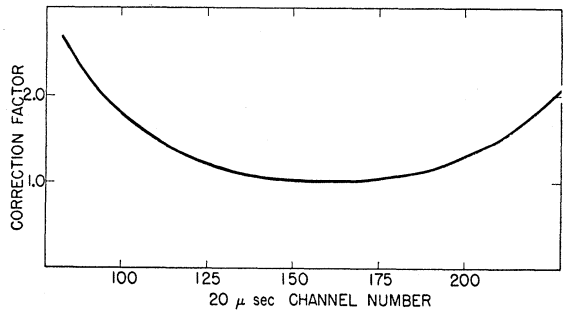

FIG. 3. Correction factor that is applied to observed neutron spectrum. It includes effects of chopper function, detector efficiency, air attenuation, and sample thickness.

[7] G. L. Squires, Proc. Roy. Soc. (London) **A212**, 192 (1952).

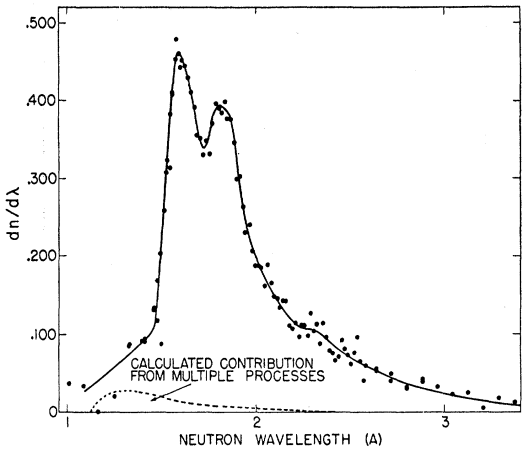

FIG. 4. Spectrum of neutrons inelastically scattered from vanadium, obtained from results of Fig. 2 by subtraction of thermal contamination and multiplication by the correction factor of Fig. 3. The dashed line is the calculated contribution from two-phonon interactions and multiple scattering in the vanadium sample.

phonon interactions to the higher of the two peaks in the scattered spectrum was computed. Another contribution of about 1.5% was estimated for multiple scattering processes in the sample for that energy. The spectral shape of these effects is calculated by approximating the lattice vibration spectrum with a simple Debye curve. The calculated neutron distribution resulting from these calculations is shown as a dashed line in Fig. 4. Because of these sources of neutrons at the high-energy end of the spectrum, the intensity is not very well determined experimentally, and may include extraneous effects.

IV. FREQUENCY DISTRIBUTION OF LATTICE VIBRATIONS

For a monochromatic incident beam of neutrons, the phonon frequency is simply related to the scattered neutron wave number by Eq. (1); hence the measured energy spectrum could be simply converted to $g(\omega)$ in that case. The results of such a calculation for the experimental spectrum of Fig. 4, assuming a single incident energy equal to the average of the real distribution, are shown in Fig. 5. The frequency, $\nu=\omega/2\pi$, is here used rather than the angular frequency ω of Eq. (1). The calculated contributions from two-phonon and multiple scattering, shown by the dashed line in Fig. 4, were subtracted before making the calculation of the frequency spectrum.

Unfortunately, the finite energy spread of the incident neutrons necessitates a correction to the frequency spectrum of Fig. 5. This correction, which cannot be computed exactly because it depends on the frequency spectrum, is described in Appendix II. It gives the results shown by the dashed line of Fig. 5. Although the actual frequency distribution probably has more detailed structure, the distribution of Fig. 5 is the most detailed that can be inferred from this experiment.

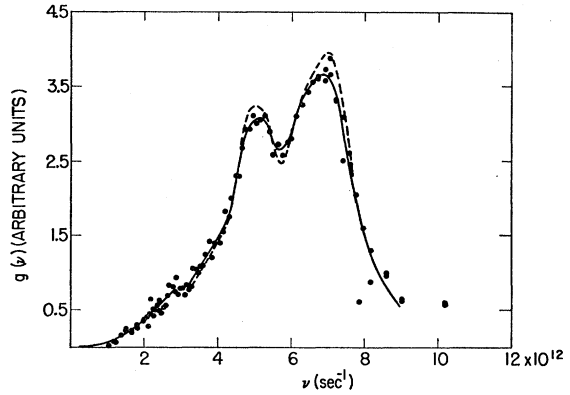

FIG. 5. The lattice vibration spectrum of vanadium. The solid line is the spectrum obtained by assuming a monochromatic incident neutron beam, and the dashed line shows the correction for the actual energy distribution of the incident beam.

The experimental frequency distribution, which contains a well resolved double peak, clearly has more structure than predicted by the simple Debye approximation of the vibration spectrum. We therefore compare our results with more recent treatments of the subject using the Born-Von Kármán theory of lattice vibrations.[8] These treatments[9–13] differ in the physical approximations used in simplifying the equations of motion of the crystal atoms.

Several authors have discussed discontinuities in slope to be expected in the frequency distribution of a three dimensional crystal. General theorems were developed by Van Hove[9] for predicting the number and type of these singularities. Specific calculations were made for a simple cubic lattice by Newell[10] and for a body-centered cubic lattice by Rosenstock and Newell.[11] The experimentally determined spectrum of Fig. 5, with two peaks of approximately equal intensities, agrees with the calculations of Fine[12] and Montroll and Peaslee[13] for body-centered cubic lattices. The ratio of the frequencies corresponding to the two peaks of the experimental curve also agrees well with the predictions for a body-centered cubic lattice, although no calculations have been carried out specifically for vanadium.

The experimental curve also gives some information about the nature of atomic forces in the vanadium lattice. If the assumption of central forces between nearest and next-nearest neighbors is justified, then the ratio of peak heights, together with the calculations of Montroll and Peaslee,[13] indicates that $\alpha \approx 4\gamma$, where α is the nearest and γ the next-nearest neighbor force constant. However, the shape of the peaks differs sufficiently from that predicted by the central-force model to warrant further calculations using noncentral forces. The effect of noncentral forces on the shape has been demonstrated by Rosenstock and Newell[11] for the simple cubic lattice.

In conclusion, the present results are generally consistent with the predictions of the Born-von Kármán theory of lattice vibrations. A more sensitive comparison with the theory awaits a specific calculation of the lattice vibrations of vanadium, however. In setting up the calculations using general forces, as discussed above it is desirable to know the elastic constants, which are not available as yet.

APPENDIX I. CORRECTIONS FOR SAMPLE THICKNESS

Because of the use of a relatively thick sample (~12.5 mm) to increase intensity and the varying cross section of vanadium over the incident spectrum, it was necessary to correct for distortion of the spectrum shape. The calculation for the arrangement is shown in Fig. 6.

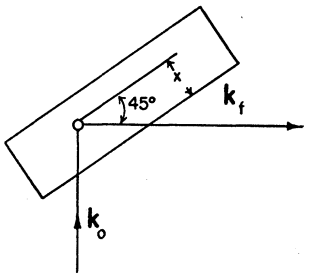

FIG. 6. Geometry of sample for calculation of effects arising from finite sample thickness.

The primary flux at a distance x into the crystal for a given incident wave number k_0 is given by

$$I_x(k_0) = I_0(k_0) \exp[-\sqrt{2}\sigma_T(k_0)Nx], \quad (3)$$

where N is the number of vanadium atoms per cc, and $\sigma_T(k_0)$ is the total cross section. If one assumes that the neutron interacts at a depth x with an inelastic cross section $\sigma_{in}(k_0,k_f)$, the flux of neutrons of final wave number k_f will be proportional to

$$I_x'(k_0,k_f) = I_x(k_0)\sigma_{in}(k_0,k_f) \exp[-\sqrt{2}\sigma_a(k_f)Nx]. \quad (4)$$

It is assumed that only the absorption cross section $\sigma_a(k_f)$ is effective in removing neutrons from the emerging beam (as there will be as many scattered into the beam as scattered out). Integrating this expression over the sample thickness and noting that the sample is thick, we obtain the flux of neutrons inelastically scattered from wave number k_0 to wave number k_f:

$$I'(k_0,k_f) \sim \frac{I_0(k_0)\times\sigma_{in}(k_0,k_f)}{[\sigma_T(k_0)+\sigma_a(k_f)]}. \quad (5)$$

The scattered flux integrated over the energy spread of

[8] M. Born and T. von Kármán, Physik. Z. **13**, 297 (1912); **14**, 15 (1913).
[9] L. Van Hove, Phys. Rev. **89**, 1189 (1953).
[10] G. F. Newell, J. Chem. Phys. **21**, 1877 (1953).
[11] H. B. Rosenstock and G. F. Newell, J. Chem. Phys. **21**, 1608 (1953).
[12] P. C. Fine, Phys. Rev. **56**, 355 (1939).
[13] E. W. Montroll and D. C. Peaslee, J. Chem. Phys. **12**, 98 (1944).

the incident beam is given by

$$I'(k_f)=\int_0^{(k_0)_{\max}} I'(k_0,k_f)dk_0 \sim\int_0^{(k_0)_{\max}} \frac{I_0(k_0)\sigma_{\text{in}}(k_0,k_f)}{[\sigma_T(k_0)+\sigma_a(k_f)]}dk_0. \quad (6)$$

In order to simplify the relationship between $I(k_f)$ and $\sigma_{\text{in}}(k_0,k_f)$ for a numerical calculation, we first rewrite the integral as

$$I(k_f)\sim\int \frac{I(k_0)\sigma_{\text{in}}(k_0,k_f)/\sigma_T(k_0)}{1+[\sigma_a(k_f)/\sigma_T(k_0)]}dk_0.$$

Since $\sigma_a(k_f)<\sigma_T(k_0)$ over most of the range of wave numbers, we assume an average value of $\sigma_T(k_0)$ in the denominator. Then

$$[\sigma_a(k_f)+\langle\sigma_T(k_0)\rangle_{\text{Av}}]I(k_f) \sim\int \frac{\langle\sigma_T(k_0)\rangle_{\text{Av}}}{\sigma_T(k_0)}I(k_0)\sigma_{\text{in}}(k_0,k_f)dk_0, \quad (7)$$

where $\langle\sigma_T(k_0)\rangle_{\text{Av}}$ is a suitable average cross section for the incident flux. The thin sample scattered spectrum was therefore obtained by correcting the observed spectrum by the factor $[\sigma_a(k_f)+\langle\sigma_T(k_0)\rangle_{\text{Av}}]$. The filtering of the incident flux in the sample was taken into account by modifying the incident flux distribution by $\langle\sigma_T(k_0)\rangle_{\text{Av}}/\sigma_T(k_0)$ when calculating the frequency spectrum.

APPENDIX II. CALCULATION OF LATTICE VIBRATION SPECTRUM FROM SCATTERED NEUTRON SPECTRUM

The cold neutron beam produces a scattered neutron spectrum given by

$$\frac{d^2N}{d\Omega dk}=\int\frac{d^2\sigma_{\text{inc}}}{d\Omega dk}(k_0,k)\varphi(k_0^2)dk_0^2, \quad (8)$$

where $\varphi(k_0^2)dk_0^2$ is the incident flux distribution. The integral is taken over k_0^2 for convenience in numerical integration. The incoherent elastic cross section for a monoenergetic incident beam of wave number k_0 is given by

$$\frac{d^2\sigma_{\text{inc}}}{d\Omega dk}(k_0,k) \sim\frac{k^2(k^2+k_0^2)\exp[-\langle U_0^2\rangle_{\text{Av}}(k^2+k_0^2)]g(k^2-k_0^2)}{k_0(k^2-k_0^2)\{\exp[h^2(k^2-k_0^2)/2mkT]-1\}}. \quad (9)$$

The factor $\exp[-\langle U_0^2\rangle_{\text{Av}}(k^2+k_0^2)]$ is the simple form of the Debye-Waller factor for scattering at 90° from a cubic crystal. The value of $\langle U_0^2\rangle_{\text{Av}}$ calculated for an assumed Debye temperature of 370° was 0.01 A².[14] Rewriting the differential spectrum of scattered neutrons as

$$\frac{dN}{d\lambda}(k^2)\sim\int_0^{(k_0)_{\max 2}}F(k^2,k_0^2)g(k^2-k_0^2)\varphi(k_0^2)dk_0^2, \quad (10)$$

one can get an approximate solution $g_1(\omega)$ by assuming a monochromatic incident beam with an effective energy $\tilde{k}_0^2$. If $\tilde{k}_0^2$ is defined by the equation

$$F(k^2,\tilde{k}_0^2)=\frac{\int F(k^2,k_0^2)\varphi(k_0^2)dk_0^2}{\int\varphi(k_0^2)dk_0^2}, \quad (11)$$

$\tilde{k}_0^2$ turns out to be constant over a large range of k^2 values. Then, approximating $\varphi(k_0^2)$ in Eq. (10) by $\delta(k^2-k_0^2)$,

$$g_1(\omega)=g_1(k^2-\tilde{k}_0^2)\sim\frac{dN}{d\lambda}(k^2)\Big/F(k^2,\tilde{k}_0^2). \quad (12)$$

Interaction of the actual incident beam with this g_1, however, would produce a neutron spectrum somewhat different from that which is observed. This can be shown by substituting g_1 in Eq. (10) and calculating the neutron spectrum, $[dN(k^2)/d\lambda]_{\text{calc}}$. We therefore try to infer a more accurate $g(\omega)$ by repeating the above procedure. We define

$$D(k^2)\equiv\left[\frac{dN}{d\lambda}(k^2)\right]_{\text{exp}}-\left[\frac{dN}{d\lambda}(k^2)\right]_{\text{calc}}=\int F(k^2,k_0^2) \times[g(k^2-k_0^2)-g_1(k^2-k_0^2)]\varphi(k_0^2)dk_0^2. \quad (13)$$

Approximating the incident beam by a δ-function as before, we obtain

$$D(k^2)=F(k^2,\tilde{k}_0^2)[g_2(k^2-\tilde{k}_0^2)-g_1(k^2-\tilde{k}_0^2)], \quad (14)$$

and

$$g_2(k^2)=g_1(k^2)+\frac{\left[\frac{dN}{d\lambda}(k^2+\tilde{k}_0^2)\right]_{\text{exp}}-\left[\frac{dN}{d\lambda}(k^2+\tilde{k}_0^2)\right]_{\text{calc}}}{F(k^2+\tilde{k}_0^2,\tilde{k}_0^2)}. \quad (15)$$

When this frequency distribution is substituted in Eq. (10) and numerically integrated, the calculated neutron spectrum agrees within statistics of the experiment with the experimental neutron spectrum.

[14] A. H. Compton and S. K. Allison, *X-Rays in Theory and Experiment* (D. Van Nostrand Company, New York, 1935), p. 438.